Widely tunable and ultrasensitive leaky-guided multimode fiber interferometer based on refractive-index-matched coupling

Cheng-Ling Lee[1,*], Kuo-Hsiang Lin[1], YuanYao Lin[2], and Jui-Ming Hsu[1]

[1]*Department of Electro-Optical Engineering, National United University, Miaoli, 360, Taiwan*

[2]*Institute of Photonics Technologies, National Tsing-Hua University, Hsinchu, 300, Taiwan*

**Corresponding author: cherry@nuu.edu.tw*

Received November 2, 2011; revised December 1, 2011; accepted December 3, 2011;
posted December 6, 2011 (Doc. ID 157414); published January 19, 2012

This investigation presents a simple, widely tunable, and ultrasensitive sensor that is based on a leaky-guided multimode fiber interferometer (MMFI) operated under refractive-index-matched coupling. By use of a material with an appropriate dispersion profile around the MMFI as a cladding yields strong index-matched coupling, which performs ultrasensitive sensing in variations of the surroundings. Index matching at a single wavelength yields a coupling wavelength dip with a narrow bandwidth and a high extinction ratio of over 25 dB. The wavelength dip can also be effectively tuned, greatly shifting with a variation in temperature (T) or refractive index (RI), when the index-matched condition is satisfied. This work demonstrates that the proposed sensor responds sensitively to T with an extremely high tuning efficiency of 50 nm/°C and an excellent sensitivity to RI of 113,500 nm per RI unit.

OCIS codes: 060.2370, 060.2310, 060.2340, 350.2460.

Numerous in-line multimode fiber interferometers (MMFIs) that use many smart and hybrid structures have been developed for a wide range of practical applications for biosensing, chemical sensing, and various types of physical parametric sensing, owing to the simplicity of their optical scheme, very low cost, good sensitivity, and high temperature stability [1–10]. MMFIs have been utilized extensively to monitor temperature (T) [2], refractive index (RI) [3], displacement [4], pressure [5], liquid level [6], and other properties [7–10]. The structures used in the MMFIs are generally based on single-mode fiber (SMF) splicing a section of no-core fiber (NCF) or multimode fiber (MMF). The interference mechanism of the MMFI is according to the reimaging theory in the NCF or MMF regions of the structures [1,11]. The fundamental mode that inputs from the SMF and propagates into the NCF can excite many multimodes (high-order cladding modes) that undergo internal total reflection (ITR) and converge in a manner determined by the reimaging, to form alternating constructive/destructive interference in the NCF by superposition of waves. The reimaging theory still applies a leaky fiber waveguide, even when the surrounding RI exceeds that of the NCF due to Fresnel reflection (FR) between the interfaces. The leaky-guided phenomenon in long-period fiber gratings (LPFGs) of the leaky waveguides has been discussed in [12–13].

This Letter presents a novel weakly guided/index-matched/leaky-guided MMFI for widely tunable filtering and ultrasensitive sensing applications. The developed device exploits appropriate cladding around the MMFI to support three properties (weakly guided, index matched, and leaky guided) in the device when a broadband light source launches, as shown in Fig. 1. Figure 1 schematically depicts the mechanism of the propagation of broadband light under (a) the weakly guided condition ($n_{\mathrm{NCF}} > n_s$) with a wavelength of λ_1 undergoing ITR, (b) the index-matched condition ($n_{\mathrm{NCF}} = n_s$) at a wavelength of λ_2, and (c) the leaky-guided condition ($n_{\mathrm{NCF}} < n_s$), with a wavelength of λ_3 under FR. The proposed configuration can perform a strong index-matched coupling to cause a high loss of single resonance at $\lambda_2(= \lambda_p)$ over a wide range of measured wavelengths. Experimental results also demonstrate that the resonant dip of the index-matched wavelength (λ_p) can be widely tuned from 1250 to 1650 nm and that the device is ultrasensitive to variations in the T or RI of the environment.

Figure 2 presents material dispersion profiles of RI for the NCF (n_{NCF}) and the cladding (n_s) used in the proposed MMFI. The two dispersion profiles of the RI intersect at a wavelength λ_p of 1440 nm, at which the RI-matching condition is satisfied. This λ_p divides the spectral range into two wavelength regions: weakly guided ($n_{\mathrm{NCF}} > n_s$) and leaky guided ($n_{\mathrm{NCF}} < n_s$). The optical properties of light that propagates in these two regions are quite different. The intensity of light that propagates along the z axis inside the NCF can be simulated using the numerical finite-difference beam propagation method (FDBPM) [4]. The three insets in Fig. 2 display the simulated results for optical intensity under the conditions of (a) weak guiding at $\lambda = 1250$ nm, (b) index matching at $\lambda_p = 1440$ nm, and (c) leaky guiding at $\lambda = 1650$ nm inside the 1 cm NCF with cladding of n_s, whose profile (dashed curve) is shown in Fig. 2. In inset (a),

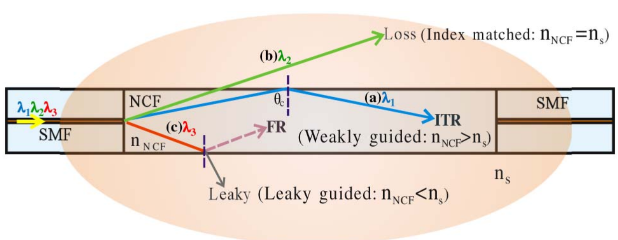

Fig. 1. (Color online) Proposed MMFI under incident broadband light with (a) λ_1, weakly guided ($n_{\mathrm{NCF}} > n_s$); (b) λ_2, index-matched ($n_{\mathrm{NCF}} = n_s$); and (c) λ_3, leaky-guided ($n_{\mathrm{NCF}} < n_s$) conditions.

0146-9592/12/030302-03$15.00/0

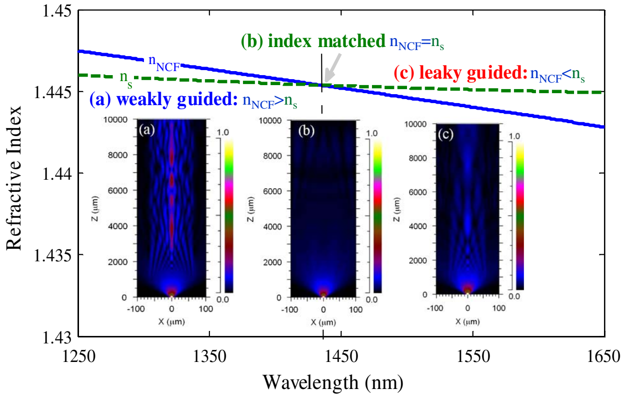

Fig. 2. (Color online) Refractive index dispersion profiles of silica NCF (n_{NCF}) and surrounding claddings (n_s). Insets show FDBPM-simulated intensities of light that propagates along the z axis inside the proposed MMFI under (a) the weakly guided condition with $n_{NCF} > n_s$, $\lambda = 1250$ nm, (b) the index-matched condition with $n_{NCF} = n_s$, $\lambda_p = 1440$ nm, and (c) the leaky-guided condition with $n_{NCF} < n_s$ at $\lambda = 1650$ nm.

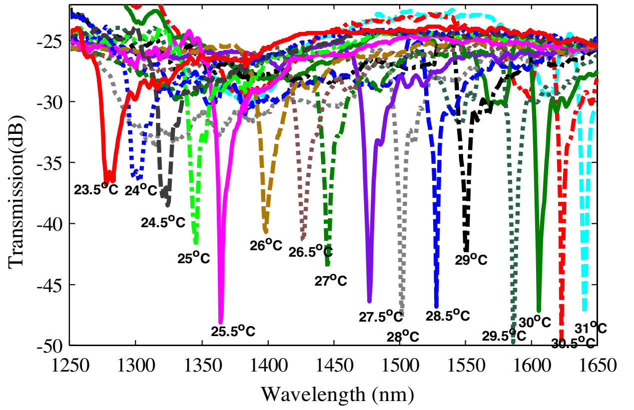

Fig. 4. (Color online) Shift of λ_p with varying T for the proposed MMFI with $L = 3.6$ cm.

many waves that undergo multiple ITRs converge mostly along the optical axis of the NCF region in the waveguide. In the leaky-guided situation with long λ, presented in inset (c), cladding modes that undergo successive FRs with various longitudinal distances at the interface between the NCF and the surroundings are reflected back to NCF with leaky loss at each FR. Inset (c) reveals that the light intensities are superimposed in the NCF region but are weaker than in (a). Under the specific condition of index matching with $n_s = n_{NCF}$ at $\lambda = 1440$ nm, waves that fully transmit along different paths into the surroundings no longer return to the NCF, as displayed in Fig. 1(b), causing very great loss at that wavelength (λ_p).

To investigate the optical characteristics of RI-matched coupling and the sensing capabilities of the developed MMFI sensor, Cargille index-matched oil ($n_D = 1.456$) is used as the cladding (n_s). Its dispersion profile of RI intersects that of silica NCF (n_{NCF}) at around $\lambda = 1340$ nm when $T = 25\,°\mathrm{C}$. A superwideband light source that comprises a set of superluminescent light emitting diodes that cover a range of wavelengths of 1250–1650 nm is employed as an optical source to launch light into the device. Figure 3 shows the shifts in the spectral responses of λ_p, measured by an optical spectrum analyzer (OSA). The transmission spectra reveal that the use of the index-matched oil as the cladding in which the experiment is performed yields only one very strong coupling dip (λ_p), which exhibits a narrow bandwidth, a sharp edge, and wide tunability over a broadband wavelength range of approximately 380 nm as T varies. In the spectral profile in Fig. 3, within the range of wavelengths shorter than λ_p ($\lambda < \lambda_p$), that associated with weak guiding $n_s < n_{NCF}$, the transmission is high because of the ITR in the waveguide, but the loss is still 10–17 dB owing to large losses of the evanescent field in the cladding modes. The evanescent fields in this weakly guided waveguide are greatly stretched into the surroundings since n_s (cladding) is close to n_{NCF} (core). The spectral range in the leaky-guided situation of wavelengths longer than $\lambda_p(\lambda > \lambda_p)$, in which n_s exceeds n_{NCF}, still exhibits reimaging because of the FR, but a greater loss of 20–25 dB is found. The results also demonstrate that the λ_p exhibits an extremely high coupling loss (> -50 dB) with a narrowband and an extinction ratio (ER) of over 25 dB (resolution of OSA: 0.8 nm). When the applied temperature $T\,(°\mathrm{C})$ is controlled using a TE cooler (resolution : $\pm\,0.05\,°\mathrm{C}$) and increased in increments of $0.5\,°\mathrm{C}$ to reduce the RI of the surrounding cladding, whose thermo-optic coefficient $dn_D/dT = -3.74\times 10^{-4}\,°\mathrm{C}^{-1}$, the λ_p varies greatly and linearly to the long wavelength side with high tunability. A higher coupling dip with a narrower bandwidth and greater ER is predicted to be realized by the use of cladding with a flatter

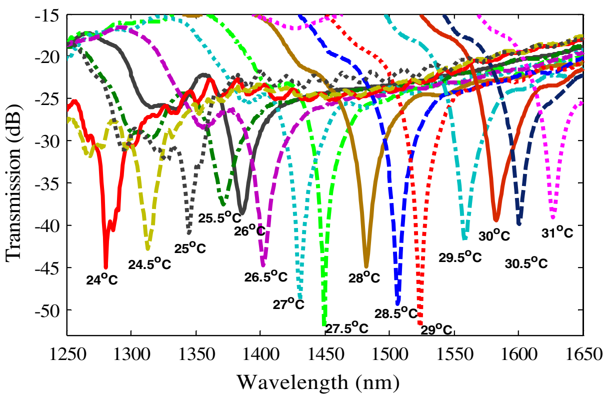

Fig. 3. (Color online) Shift of λ_p with varying T for the proposed MMFI with $L = 1.0$ cm.

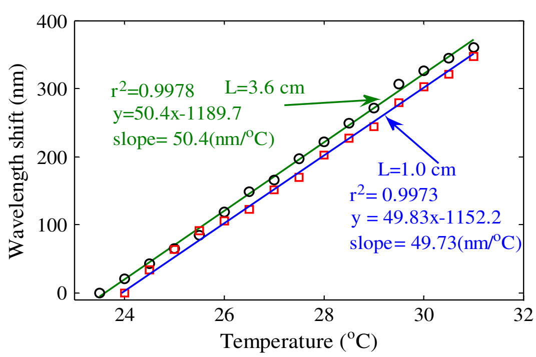

Fig. 5. (Color online) Temperature sensitivities and tuning efficiencies of MMFI sensors with $L = 1.0$ cm and 3.6 cm.

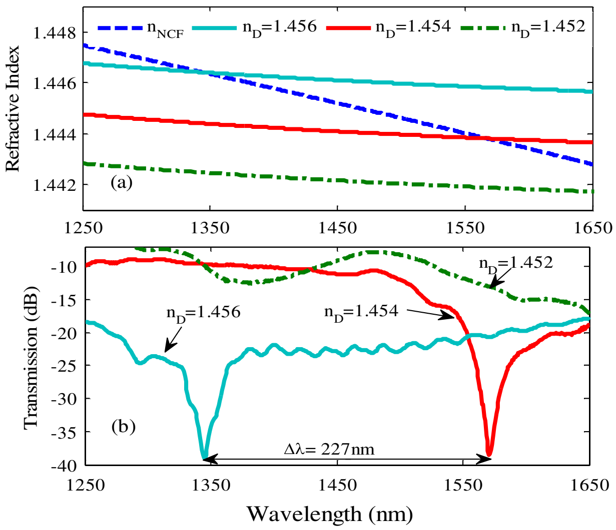

Fig. 6. (Color online) (a) RI dispersion profiles of n_{NCF} and claddings with different Cargille index-matched oils, and (b) spectral responses of proposed 1 cm MMFIs with n_s of $n_D = 1.456$, 1.454, and 1.452 at fixed 25 °C.

dispersion slope, since a larger angle of intersection between the two dispersion profiles is associated with compression of the transition from weakly guided to leaky-guided regions, abruptly yielding a large index-matched loss.

The proposed MMFI can easily be multiplexed by arbitrarily selecting NCF with different length. The MMFI with a long length of 3.6 cm provides a much narrower bandwidth of wavelength dips to increase the resolution of measurement. However, it presents a high loss in the transmission spectra, as shown in Fig. 4. Figure 5 presents the similar sensing performance of MMFIs with different lengths. Experimental results demonstrate that the T sensitivity and tuning efficiency of λ_p in the two MMFIs are similar, since the temperature sensing performance is dominated by the thermo-optic coefficient of the surroundings. T sensitivity and tuning efficiency of as high as 50 nm/°C are achieved using the proposed sensing configuration.

In fact, the T sensitivity of the MMFI sensor in the study [2] is inherently low since the T sensitivity is controlled by the thermal expansion coefficient (~$5\times 10^{-7}\,°\mathrm{C}^{-1}$) and the thermo-optic coefficient (10^{-5}–$10^{-6}\,°\mathrm{C}^{-1}$) of the silica fiber. Hence, the T sensitivity was proportional to $[(n+\Delta n)\cdot(D+\Delta D)^2]/(L+\Delta L)]$, where n, D, and L represent the RI, diameter, and NCF length, and the measured T sensitivity was only 0.0129 nm/°C [2]. However, the T sensitivity in our work is much greater improved because the sensing mechanism of the developed sensor is based on index-matched coupling by use of dispersion engineering in the device. Therefore, the sensor presented here differs greatly from the sensor in the cited work [2]. Various media can be used as surroundings if their dispersion profiles satisfy the criteria for index matching.

To evaluate the measurement of RI of the external medium by the proposed sensing mechanism, index-matched oils with RI values of $n_D = 1.456$, 1.454, and 1.452 (intervals 0.002) are utilized as the surrounding media (n_s) at fixed $T = 25\,°\mathrm{C}$. Figure 6(a) shows the theoretical intersecting wavelengths of around 1345 and 1575 nm for the external surroundings with $n_D = 1.456$ and 1.454, respectively. Clearly, the lack of any intersection between the two profiles with n_{NCF} and $n_D = 1.452$ indicates the absence of index-matched coupling. The spectral responses and sensitivities are measured, as shown in Fig. 6(b), and the λ_p shifts more than 227 nm as the RI changes only 0.002. These results demonstrate that the excellent sensitivity of the sensor may be as high as $(227)/0.002 = 113{,}500$ nm/RI units (RIU) although only values of RI that are close to those of the sensor can be measured.

In conclusion, this work demonstrated a very simple, cost-effective, widely tunable, and ultrasensitive sensor based on index-matched coupling in a leaky-guided MMFI with appropriate material dispersion engineering. The high thermo-optic coefficient of the index-matched oil around the proposed MMFI substantially improves the T sensitivity and tunability. Experimental results also show an excellent RI sensitivity of about 113,500 nm /RIU when the RI is within the range of $n_D = 1.454$–1.456. The configuration of the sensor can yield superior characteristics of an abrupt and high ER, narrow bandwidth, and a single wavelength dip over a wide range of wavelengths. The novel device can be utilized as an ultrasensitive sensor of temperature, RI, or concentration of a solution for biochemical technology.

This research is supported by the National Science Council of the Republic of China, NSC 98-2221-E-239-002-MY2.

References

1. L. B. Soldano and E. C. M. Pennings, J. Lightwave Technol. **13**, 615 (1995).
2. J. G. Aguilar-Soto, J. E. Antonio-Lopez, J. J. Sanchez-Mondragon, and D. A. May-Arrioja, J. Phys. Conf. Ser. **274**, 012011 (2011).
3. Y. Jung, S. Kim, D. Lee, and K. Oh, Meas. Sci. Technol. **17**, 1129 (2006).
4. A. Mehta, W. Mohammed, and E. Johnson, IEEE Photon. Technol. Lett. **15**, 1129 (2003).
5. V. I. Ruiz-Pérez, M. A. Basurto-Pensado, P. LiKamWa, J. J. Sánchez-Mondragón, and D. A. May-Arrioja, J. Phys. Conf. Ser. **274**, 012025 (2011).
6. J. E. Antonio-Lopez, J. J. Sanchez-Mondragon, P. LiKamWa, and D. A. May-Arrioja, Opt. Lett. **36**, 3425 (2011).
7. J. E. Antonio-Lopez, A. Castillo-Guzman, D. A. May-Arrioja, R. Selvas-Aguilar, and P. LiKamWa, Opt. Lett. **35**, 324 (2010).
8. W. S. Mohammed, P. W. E. Smith, and X. Gu, Opt. Lett. **31**, 2547 (2006).
9. S. Shaklan, F. Reynaud, and C. Froehly, Appl. Opt. **31**, 749 (1992).
10. A. Castillo-Guzman, J. E. Antonio-Lopez, R. Selvas-Aguilar, D. A. May-Arrioja, J. Estudillo-Ayala, and P. LiKamWa, Opt. Express **18**, 591 (2010).
11. W. S. Mohammed, A. Mehta, and E. G. Johnson, J. Lightwave Technol. **22**, 469 (2004).
12. D. B. Stegall and T. Erdogan, IEEE Photon. Technol. Lett. **11**, 343 (1999).
13. C.-L. Lee, Z.-Y. Weng, C.-J. Lin, and Y.-Y. Lin, Opt. Lett. **35**, 4172 (2010).